

# The Effects of Photoionization on Galaxy Formation — II: Satellite Galaxies in the Local Group

A. J. Benson<sup>1</sup>, C. S. Frenk<sup>2</sup>, C. G. Lacey<sup>3</sup>, C. M. Baugh<sup>2</sup> & S. Cole<sup>2</sup>

1. *California Institute of Technology, MC 105-24, Pasadena, CA 91125, U.S.A. (e-mail: abenson@astro.caltech.edu)*

2. *Physics Department, University of Durham, Durham, DH1 3LE, England*

3. *SISSA, Astrophysics Sector, via Beirut 2-4, 34014 Trieste, Italy*

30 October 2018

## ABSTRACT

We use a self-consistent model of galaxy formation and the evolution of the intergalactic medium to study the effects of the reionization of the universe at high redshift on the properties of satellite galaxies like those seen around the Milky Way. Photoionization suppresses the formation of small galaxies, so that surviving satellites are preferentially those that formed before the universe reionized. As a result, the number of satellites expected today is about an order of magnitude smaller than the number inferred by identifying satellites with subhalos in high-resolution simulations of the dark matter. The resulting satellite population has an abundance and a distribution of circular velocities similar to those observed in the Local Group. We explore many other properties of satellite galaxies, including their gas content, metallicity and star formation rate, and find generally good agreement with available data. Our model predicts the existence of many as yet undetected satellites in the Local Group. We quantify their observability in terms of their apparent magnitude and surface brightness and also in terms of their constituent stars. A near-complete census of the Milky Way’s satellites would require imaging to  $V \approx 20$  and to a surface brightness fainter than 26 V-band magnitudes per square arcsecond. Satellites with integrated luminosity  $V = 15$  should contain of order 100 stars brighter than  $B = 26$ , with central stellar densities of a few tens per square arcminute. Discovery of a large population of faint satellites would provide a strong test of current models of galaxy formation.

**Key words:** cosmology: theory - galaxies: formation - Local Group - intergalactic medium

## 1 INTRODUCTION

High-resolution N-body simulations of the formation of dark matter halos in the cold dark matter (CDM) cosmogony reveal a large number of embedded subhalos that survive the collapse and virialization of the parent structure (Klypin et al. 1999a; Moore et al. 1999). Although their aggregate mass typically represents less than 10% of the total halo mass, these substructures are very numerous. In rich clusters, the abundance of surviving subhalos is comparable to the abundance of bright galaxies. In galaxy halos, on the other hand, the number of subhalos exceeds the number of faint satellites observed in the Local Group by well over an order of magnitude. This discrepancy has recently been highlighted as a major flaw of the CDM cosmogony and has prompted investigation of alternative cosmological models. These range from non-standard models of inflation (Kamionkowski & Liddle 2000) to models in which the universe is dominated by warm, self-interacting or annihilating dark matter which may not generate small-scale substructure in galactic halos, but may do so on cluster scales (Hogan

1999; Spergel & Steinhardt 2000; Moore 2000; Yoshida et al. 2001; Craig & Davis 2001).

That hierarchical clustering theories predict many more small dark matter halos than there are faint galaxies in the local universe has been known for a long time, as has one possible solution to this apparent conflict (White & Rees 1978). Feedback generated by the energy injected into galactic gas in the course of stellar evolution can regulate star formation in small halos rendering their galaxies too faint to be detected in local surveys (White & Rees 1978; Dekel & Silk 1986; Cole 1991; White & Frenk 1991; Lacey & Silk 1991). The overabundance of dark subhalos around the Milky Way predicted by CDM models was also known before the high resolution N-body simulations highlighted the discrepancy (Kauffmann, White & Guiderdoni 1993). Using a semi-analytic model of galaxy formation based on the extended Press-Schechter theory for the assembly histories of dark halos (Bond et al. 1991; Bower 1991), Kauffmann et al. recognized the Milky Way “satellite” problem and examined various possible solutions (see their Fig. 1). They concluded that the best way to reconcile their models with the luminosity function of the Milky Way’s satellites was to

arXiv:astro-ph/0108218v1 13 Aug 2001

assume that gas is unable to cool within dark matter halos of circular velocity less than  $150 \text{ km s}^{-1}$  at redshifts between 5 and 1.5. They suggested that this effect might result from a photoionizing background at high redshift, but also noted that the required suppression threshold of  $150 \text{ km s}^{-1}$  was much larger than was expected based on physical calculations of the effects of photoionization. Moore (2001) has expanded on the reasons why standard supernova feedback of the kind invoked to explain the relative paucity of faint field galaxies in CDM models does not, on its own, solve the Milky Way satellite problem. He points out that the observed satellites of the Milky Way of a given abundance have circular velocities which are about three times smaller than the circular velocities of subhalos of the same abundance in the N-body simulations.

The lack of a Gunn-Peterson effect in the spectra of high redshift quasars indicates that the Universe was reionized at  $z \gtrsim 6$  (Fan et al. 2000). The reionization of the universe raises the entropy of the gas that is required to fuel galaxy formation, preventing it from accreting onto small dark matter halos and lengthening the cooling time of that gas which is accreted. The inhibiting effects of photoionization have been investigated in some detail (Rees 1986; Babul & Rees 1992; Efstathiou 1992; Shapiro, Giroux & Babul 1994; Katz, Weinberg & Hernquist 1996; Quinn, Katz & Efstathiou 1996; Thoul & Weinberg 1996; Abel & Mo 1997; Kepner, Babul & Spergel 1997; Weinberg, Hernquist & Katz 1997; Navarro & Steinmetz 1997; Barkana & Loeb 1999), with the conclusion that galaxy formation is strongly suppressed by reionization in halos of circular velocity,  $V_C \lesssim 60 \text{ km s}^{-1}$ . Although this value is smaller than the value assumed by Kauffmann, White & Guiderdoni (1993), their general picture remains valid: the number of satellites around bright galaxies is much smaller than the number of dark matter subhalos because only those subhalos that were already present before reionization were able to acquire gas and host a visible galaxy. This idea has recently been investigated further by Bullock, Kravtsov & Weinberg (2000). These authors followed the formation of dark halos using a merger tree formalism similar to that of Kauffmann, White & Guiderdoni (1993), but taking into account the tidal effects experienced by substructures when they are accreted into their parent halo. Combining their halo model with a simple argument based on the mass-to-light ratio of satellite galaxies, they calculated their observability, concluding that, for a reasonable redshift of reionization, the number of visible satellites would indeed be close to that observed. A similar conclusion was reached by Somerville (2001) using a semi-analytic model similar to that of Cole et al. (2000) but with more limited model of photoionization than used in this work (specifically, the model use by Somerville (2001) does not self-consistently evolve the properties of galaxies and the IGM and does not account for the effects of photoheating of virialized gas in halos or tidal disruption of satellites).

In this paper, we investigate the abundance and properties of satellite galaxy populations using a model of galaxy formation which self-consistently calculates the physics of reionization and the process of galaxy formation. We use the semi-analytic techniques developed by Cole et al. (2000) which we have recently extended to enable calculation of the coupled evolution of the intergalactic medium (IGM) and galaxies (Benson et al. 2001; hereafter Paper I). The model

follows the formation and evolution of stars, the production of ionizing photons from stars and quasars, the reheating of the IGM, and the associated suppression of galaxy formation in low mass halos. The model also incorporates a detailed treatment of the dynamics of satellite halos under the influence of dynamical friction and tidal forces. Like the halo model of Bullock, Kravtsov & Weinberg (2000), our model agrees with the results of the high-resolution N-body simulations. In Paper I, we demonstrated that reionization reduces the number of faint field galaxies in the local Universe, flattening the faint end slope of the galaxy luminosity function, in good agreement with the most recent observational determinations. In this paper, we will explore the properties predicted by this very same model (i.e. with the same parameter values) for the population of satellites around galaxies like the Milky Way. We will carry out as detailed a comparison as is possible with current observational data and present tests of our model which rely on the prediction of a large and as yet undetected population of faint satellites in the halo of the Milky Way.

The remainder of this paper is organised as follows. In §2, we briefly describe our model. In §3, we calculate the expected luminosity function and circular velocity function of satellites around galaxies like the Milky Way. In this section, we also discuss observational strategies for discovering the large faint satellite population predicted by our model. In §4, we compare the gas content, star formation rate, metallicity and structure of our model satellites with observational data. Finally, in §5 we present our main conclusions.

## 2 MODEL

We begin by briefly describing our model, a full description of which may be found in Paper I. We represent the IGM as a distribution of gas elements whose density evolves as a result of the expansion of the Universe and the formation of structure. Each element ‘sees’ a background of ionizing photons emitted by stars (as given by the star formation history in our model of galaxy formation) and by quasars (as obtained from the observational parametrization of Madau, Haardt & Rees 1999), which ionize and heat the gas. From this, we derive the thermal and ionization history of the IGM. The hot IGM acquires a significant pressure which hampers the accretion of gas into low mass dark matter halos. From the inferred thermal state of the IGM we derive the filtering mass, defined as the mass of a dark matter halo which accretes a gas mass equivalent to 50% of the universal baryon fraction (Gnedin 2000), as a function of time.

Knowledge of the filtering mass allows us to determine how much gas is available for galaxy formation in a given dark matter halo at any time. The increase in entropy produced by reionization causes lower mass halos to contain a smaller fraction of their mass in the form of gas than larger mass halos. The ionizing background which accumulates after reionization also heats gas already present in dark matter halos, preventing it from cooling into the star forming phase. We include this heating in our estimates of the mass of gas which can cool, resulting in a further suppression of galaxy formation. When a galaxy falls into a larger halo becoming a satellite in it, we compute its orbit through the halo in detail, accounting for the effects of dynamical friction, tidal

limitation and gravitational shocking (as described by Taylor & Babul (2000) and in Paper I). As was demonstrated in Paper I, our model of satellite dynamics reproduces the results of high-resolution N-body simulations with reasonable accuracy in both of the cosmological models for which numerical results are available.

In Paper I, we performed calculations using our extended galaxy formation model in a  $\Lambda$ CDM cosmology (mean mass density  $\Omega_0 = 0.3$ , cosmological constant term  $\Lambda/3H_0^2 = 0.7$ , mean baryon density  $\Omega_b = 0.02$ , and Hubble parameter  $h = 0.7$ .) The values of the model parameters required to describe the relevant physical processes are strongly constrained by a small subset of the local galaxy data; we showed that the model also reproduces many other properties of the galaxy population at  $z = 0$  (see also Cole et al. 2000). We will retain exactly the same parameter values throughout the present work. The result is a fully-specified model of galaxy formation that incorporates the effects of reionization and tidal limitation and which we now use to explore in detail the properties of satellite galaxies around the Milky Way.

### 3 THE ABUNDANCE OF SATELLITES

We study the population of satellite galaxies that form in an ensemble of halos harbouring galaxies similar to the Milky Way. We class a galaxy as being “similar to the Milky Way” if the circular velocity of its disk ( $V_{C,d}$ , measured at the disk half-mass radius) is between 210 and 230  $\text{km s}^{-1}$ , and if its bulge-to-total mass ratio (including stars and cold gas) is in the range 0.05 to 0.20 (which is approximately the range found by Dehnen & Binney (1998) in mass models of the Milky Way).

Using our model of galaxy formation, including all the effects of photoionization and tidal limitation described in §2, we construct 1800 realizations of dark matter halos with mass in the range  $4.0 \times 10^{11}$  to  $2.3 \times 10^{12} h^{-1} M_\odot$  (the range in which we find galaxies similar to the Milky Way) at  $z = 0$ . We ensure that our calculation resolves all halos into which gas is able to accrete and cool in the redshift interval 0 to 25. From the set of simulated halos we select those which contain a central galaxy similar to the Milky Way. We find approximately 70 such halos in our sample. These have “quieter” merger histories than is typical for halos of their mass, as was shown, for example, by Baugh, Cole & Frenk (1996). All other halos are discarded and, for the remainder of this paper, we consider only the satellite populations of halos hosting Milky Way type galaxies. We refer to this sample of satellites as our “standard model.” For comparison, we also generated a sample of Milky Way satellites using our model with no photoionization (but still including the effects of tidal limitation of satellites), which we will refer to as the “no photoionization” model, and a sample of Milky Way satellites with the original model of Cole et al. (2000), which includes neither photoionization nor tidal effects.

To test our model, we make use of observational data on Local Group galaxies taken from the compilation by Mateo (1998). Mateo points out that the census of Local Group dwarfs is almost certainly incomplete. Unfortunately, the observational selection effects are not quantitatively well understood, and so we do not attempt to correct for them here,

but note that they could possibly alter the observational results significantly. Some galaxies classed as members of the Local Group lie outside the virial radii of the dark matter halos thought to be associated with the Milky Way and M31. For the Milky Way, we can estimate the virial radius using the three-component mass models of Dehnen & Binney (1998), some of which assume dark matter halos with the NFW (Navarro, Frenk & White 1997) profile appropriate to the CDM universe that we are considering here. Of these, their model 2d gives the best fit to the observational data that they consider. Assuming a spherical top-hat collapse model for the Milky Way halo then implies a virial mass and radius of  $M_{\text{MW}} = 1.11 \times 10^{12} M_\odot$  and  $R_{\text{MW}} = 272$  kpc respectively (for the particular set of cosmological parameters considered in this paper). This is in good agreement with the virial radii of the halos that end up hosting Milky Way type galaxies in our model, which typically have  $R_{\text{vir}} \approx 300$  kpc. (The model predicts a distribution of  $R_{\text{vir}}$  because Milky Way type galaxies can be found in halos with a range of masses). Lacking any better estimate, we also take  $R_{\text{MW}}$  as the virial radius of M31, since the measured circular velocity of M31 is quite close to that of the Milky Way. Throughout this section, we will distinguish between Local Group satellites and satellites lying within  $R_{\text{MW}}$  of either the Milky Way or M31.

#### 3.1 Abundance as a function of luminosity and stellar mass

We begin by comparing the luminosity function of the population of satellites in the model with the observed luminosity function of satellites of the Local Group. Fig. 1 shows the V-band luminosity function of satellites<sup>\*</sup>, normalised to the number of central galaxies (i.e. the Milky Way and M31), as filled circles. We include only satellites within  $R_{\text{MW}}$  of either the Milky Way or M31. Throughout this paper, we use magnitudes corrected for foreground extinction by the Milky Way using the reddening values listed by Mateo (1998). The median luminosity function from all pairs of Milky Way type galaxies in our standard model is shown by the solid line, with errorbars enclosing 10% and 90% of the distribution of luminosity functions. (We calculate the median and intervals for pairs of halos since we are comparing to the combined Milky Way and M31 datasets and the scatter in model predictions for pairs of halos is, of course, smaller than for single halos.) The satellite galaxies in our model typically have only very small amounts of internal dust-extinction (all but a tiny fraction have less than 0.1 magnitudes of extinction in the V-band). Nevertheless, we include the effects of internal dust-extinction in all model magnitudes.

It is immediately apparent in Fig. 1 that photoionization does help to reduce the number of satellite galaxies: our model predicts many fewer satellites than the model of Cole et al. (2000). Furthermore, the dashed line shows that tidal stripping also acts to reduce the number of satellites of a given luminosity, but this is a much smaller effect. For  $M_V \approx -10$ , the combined effects of tidal stripping and photoionization reduce the number of satellites by about a factor of 10 compared to the Cole et al. (2000) model. Note that

\* We include the SMC, LMC and M33 in this category.

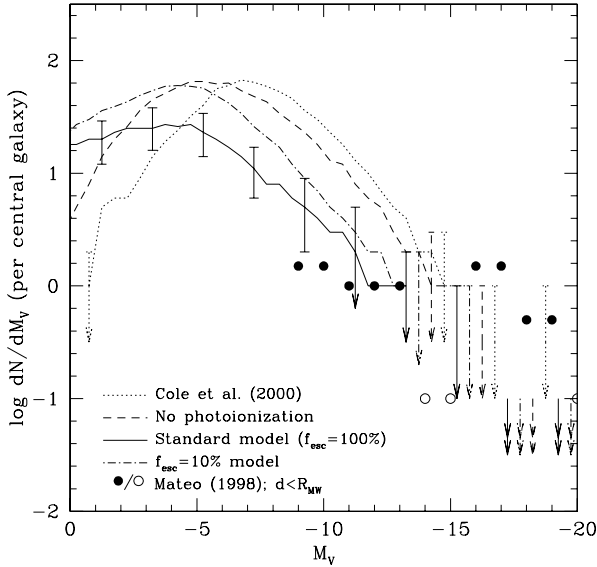


**Figure 1.** The V-band luminosity function of satellite galaxies (per central galaxy). The Local Group data, taken from the compilation of Mateo (1998), are shown as filled circles, except for bins in which the luminosity function is zero which we indicate by an open circle at arbitrary position on the y-axis (faintwards of  $M_V = -9$  there are no known satellites so we plot no symbols). Only satellites within  $R_{MW}$  of the Milky Way or M31 are included and no correction for any possible incompleteness has been applied. The median luminosity function of satellites around pairs of Milky Way type galaxies in our model is shown by the solid line, with errorbars indicating the 10% and 90% intervals of the distribution of luminosity functions found in approximately 70 realizations of the satellite galaxy population. Where the 10% interval corresponds to zero galaxies, a single-headed downward-pointing arrow is plotted. Where there is no connecting line, the median is zero, and the 90% interval is shown by an errorbar and arrow. Where the 90% interval corresponds to zero galaxies (i.e. less than one in ten of the simulated halos contained any galaxies of this magnitude), we show a double-headed downward-pointing arrow (at an arbitrary position on the y-axis). The dashed line corresponds to the model in which the effects of photoionization are ignored (but tidal limitation of satellites is included), while the dotted line shows the prediction from the model of Cole et al. (2000) and the dot-dashed line shows results from our standard model with the reduced escape fraction of  $f_{esc} = 10\%$ . For clarity we have omitted error bars from these three models; these are typically 10–20% smaller than for the standard model.

the model predicts significant variation in the satellite luminosity function from halo to halo. Once this scatter is taken into account, our standard model is in reasonable agreement with the Local Group luminosity function, except perhaps at the brightest magnitudes, where the model underpredicts the number of satellites. However, the statistics are poor at these magnitudes, because there are so few galaxies. For example, the  $-17.5 \geq M_V > -18.5$  bin in Fig. 1 contains a single galaxy (the LMC) within  $R_{MW}$ , implying a mean of 0.5 such satellites per central galaxy. Our model predicts a mean of approximately 0.08. Since no halo in the sample contains more than one such galaxy, 8% of the model halos contain a satellite galaxy in this luminosity range. Thus,

such bright satellites are not impossible in our model, but they are quite rare.

As was noted in Paper I, the disk velocity dispersion used in the Taylor & Babul (2000) model ( $\sigma_d = V_{C,d}/\sqrt{2}$ ) is rather high for the Milky Way. This quantity determines the magnitude of the dynamical friction force felt by satellites which pass close to the disk of the central galaxy, and so may affect the rate of merging for satellites on highly eccentric orbits. An overly large  $\sigma_d$  would result in a reduced dynamical friction force and a lower rate of mergers, potentially leading us to overestimate the number of satellites remaining. However, adopting the more appropriate value,  $\sigma_d = 0.2V_{C,d}$ , makes virtually no difference to the predicted number of satellites, since the disk velocity dispersion is only important for satellites very close to the central galaxy, and which therefore tend to merge shortly afterwards in any case. On the other hand, the abundance of the faintest satellites is fairly sensitive to two uncertain model assumptions, the escape fraction of ionizing photons,  $f_{esc}$ , and the luminosity of the galaxies that we have classed as resembling the Milky Way.

In Paper I, we found that adopting an escape fraction,  $f_{esc} = 100\%$  (i.e. all ionizing photons produced by stars escape from their galaxy into the IGM), results in a reasonable redshift of reionization ( $z \approx 8$ ), but also in an ionizing background which is significantly higher than current observational estimates. On the other hand, a fraction,  $f_{esc} = 10\%$ , results in a more reasonable ionizing background and is in better agreement with observational determinations of  $f_{esc}$  (Leitherer et al. 1995; Steidel, Pettini & Adelberger 2001), but implies a lower redshift of reionization ( $z \approx 5.5$ ), perhaps uncomfortably close to the lower limit imposed by the lack of a Gunn-Peterson effect in the highest redshift quasars. We find that the lower redshift of reionization associated with  $f_{esc} = 10\%$  leads to a larger number of satellites of a given luminosity (as shown by the dot-dashed line in Fig. 1), producing a luminosity function which, faintwards of  $M_V = -11$ , is a factor of about two too high compared with the data (even after allowing for halo-to-halo variations). However, possible incompleteness at the faint end of the observed luminosity function makes this comparison inconclusive. We will adopt  $f_{esc} = 100\%$  as our standard value for all results presented in this paper, unless stated otherwise.

A second source of uncertainty is the identification of model galaxies with the Milky Way. As discussed in Paper 1 (see Fig. 9), our modelling of the structure of disks is crude and produces circular velocities for spiral galaxies that are typically 30% larger for their luminosity than is implied by the observed Tully-Fisher relation. As a result, the model galaxies that we have identified with the Milky Way according to their circular velocity are somewhat fainter than galaxies lying on the mean Tully-Fisher relation at that circular velocity. We could alternatively select Milky Way galaxies according to luminosity. Direct estimates of the luminosity of the Milky Way are rather uncertain and so we instead estimate the luminosity from the observed Tully-Fisher relation as advocated by Binney & Merrifield (1998, §10.1). The observed Tully-Fisher relation (Matthewson, Ford & Buchhorn 1992) implies an I-band magnitude in the region of  $-21.5 \gtrsim M_I - 5 \log h \gtrsim -22.0$  for a typical galaxy with the circular speed of the Milky Way.

Model galaxies with I-band magnitude in this range (and bulge-to-total ratio in the range discussed above) typically have higher circular velocities, and inhabit higher mass halos than the Milky Way type galaxies of our original sample. As a result, this new sample has a substantially larger number of satellites. Its luminosity function is compatible with observations for magnitudes brighter than  $M_V \approx -13$ , but faintwards of this, it overpredicts the number of satellites. Again, possible incompleteness in the faint data makes it difficult to exclude this model, but for it to be compatible with observations, the data would have to be severely incomplete so that at least 70% of  $M_V \approx -10$  satellites should have been missed.

As can be clearly seen from Fig. 1, our model predicts that the satellite galaxy luminosity function should continue to rise at magnitudes fainter than the faintest satellite yet observed. The luminosity function peaks at  $M_V \approx -3$  and then falls off at fainter magnitudes. This cut-off is caused by the inability of gas below  $10^4\text{K}$  to cool when no molecular hydrogen is present. The cut off occurs at significantly fainter magnitudes in our standard model than in the model with no photoionization or the Cole et al. (2000) model since photoionization reduces the efficiency of galaxy formation in halos of a given mass (or, equivalently, virial temperature) making the galaxies in those halos fainter<sup>†</sup>. It is interesting therefore to consider the observability of the galaxies that make up the faint end of the satellite luminosity function. In Fig. 2 we show the number of satellite galaxies per halo as a function of their apparent V-band magnitude. To infer the distances to the satellites, we have made use of their orbital positions, assuming that they are observed from a location 8 kpc from the centre of the host halo (i.e. at about the position of the Sun in the Milky Way). (The mean distance for  $M_V \leq -10$  satellites is 95 kpc and this changes only slowly with  $M_V$ )<sup>‡</sup>. The solid line shows all satellites, while the dotted and dashed lines show only those whose central surface brightness is brighter than 26 and 22 magnitudes per square arcsecond respectively. Central surface brightnesses for model galaxies were computed using the predicted luminosities and sizes, with disk components modelled as exponential disks, and spheroids as King profiles with  $r_t/r_c = 10$ . The faintest known Local Group galaxy is Tucana ( $m_V = 15.15$  with almost no foreground extinction; note that this point is not seen in Fig. 2 since Tucana lies outside of the Milky Way’s virial radius), only slightly brighter than the peak in the predicted apparent magnitude distribution. Surface brightness adds a further limit to the detectability of satellites. Currently the lowest surface

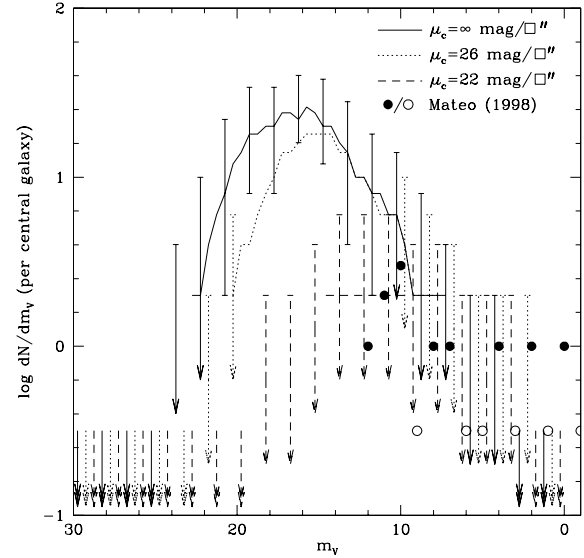


**Figure 2.** V-band number counts of satellites. The solid line shows the results from our standard model with no cut on central surface brightness, while dotted and dashed lines show the effects of applying a central surface brightness cut of 26 and 22 magnitudes per square arcsecond respectively. Lines show the median counts in the standard model, with errorbars indicating the 10% and 90% intervals of the distribution for the results with no surface brightness cut. (The errorbars for the 26 magnitudes per square arcsecond sample are comparable to these, except for  $m_V < 16$  where they are about twice as large.) Where the 10% interval corresponds to zero galaxies, a single-headed downward pointing arrow is shown. Where only an errorbar or arrow is shown (i.e. there is no connecting line), the median is zero, and where the 90% interval corresponds to zero galaxies we show a double-headed downward-pointing arrow (at arbitrary position on the y-axis). Note that unlike the luminosity function (Fig. 1), the results here refer to a single halo (as opposed to pairs of halos). Apparent magnitudes for satellites are computed from their position in the host halo, assuming the observer is located 8 kpc from the centre. The filled circles show the observed counts from Mateo (1998), including only those galaxies within  $R_{\text{MW}}$  of the Milky Way. Where a bin contains no observed satellites we show an open circle at arbitrary position on the y-axis (faintwards of the  $m_V = 12$  bin there are no observed satellites, so we do not plot any symbols).

brightness member of the Local Group that is known is Sextans, with  $\mu_0 = 26.2 \pm 0.5 \text{ mag arcsec}^{-2}$  (Mateo 1998). This is close to the dotted line in Fig. 2. It is clear from Fig. 2 that the faint satellites have very low surface brightness and that finding them will require very deep photometry.

Several satellites have now been detected as an excess of stars against the background of the Milky Way (e.g. Irwin & Hatzidimitriou 1995). From the star formation histories of our model satellites, we can calculate the number and surface density of stars visible today. We use the stellar evolutionary tracks of Lejeune & Schaerer (2001) to obtain the number of stars brighter than a certain luminosity,  $L_c$ , in a single stellar population of unit mass, as a function of age and metallicity:

<sup>†</sup> We are able to predict the properties of these very faint galaxies by extrapolating our standard rules for star formation, feedback etc. to these very small objects. However, it should be kept in mind that these very faint galaxies typically contain only a few thousand Solar masses of stars. It is not clear how well our simplified rules for star formation describe reality in such systems, where the entire galaxy is less massive than a single giant molecular cloud.

<sup>‡</sup> The number density of satellites within the virial radius of a Milky Way type halo in our model scales roughly as  $r^{-2}$  for  $r \gtrsim 10$  kpc with a rapid cut-off towards  $R_{\text{vir}}$ , but flattens significantly at smaller radii since these inner satellites are strongly affected by tidal forces and dynamical friction.

$$N_{L_c}(t, Z) = \int_{M_{\min}}^{M_{\max}} S_{L_c}(M, t, Z) \frac{dn}{dM} dM, \quad (1)$$

where  $dn/dM$  is the stellar Initial Mass Function (IMF; we use the IMF of Kennicutt (1983), as assumed in our calculations of galaxy luminosities), normalized to unit mass and with minimum and maximum masses,  $M_{\min}$  and  $M_{\max}$  ( $0.1$  and  $125M_{\odot}$  respectively), and

$$S_{L_c}(M, t, Z) = \begin{cases} 0 & \text{if } L(M, t, Z) < L_c \\ 1 & \text{if } L(M, t, Z) \geq L_c, \end{cases} \quad (2)$$

where  $L(M, t, Z)$  is the luminosity of a star of zero-age mass  $M$ , age  $t$  and metallicity  $Z$ . The number of stars more luminous than  $L_c$  in a galaxy at the present day is then given by

$$N = \int_0^{t_0} \dot{\rho}_*(t) N_{L_c}(t_0 - t, Z[t]) dt, \quad (3)$$

where  $\dot{\rho}_*(t)$  is the star formation rate in the galaxy at time  $t$  and  $Z[t]$  is the metallicity of the stars being formed at time  $t$ . For each satellite, we compute the luminosity corresponding to a given apparent magnitude limit at its position in the halo and determine  $N$ . From the known size of the disk and spheroidal component of each model galaxy, we also derive the central number density of these stars. Fig. 3 shows the result of this calculation. (We do not include the effects of dust extinction on the stellar luminosities since this varies across the galaxy, but we do include them in the total galaxy magnitude. As noted above, these internal extinction corrections are typically small in any case.) The central stellar densities predicted by our model are in excellent agreement with those measured by Irwin & Hatzidimitriou (1995) from scanned photographic plates with a limiting magnitude of  $B=22$ : compare the open stars with the open triangles in Fig. 3. Imaging two magnitudes deeper (circles) would allow the detection of galaxies to  $V=17-18$  at the same central surface density, although the higher density of background objects may make detection more difficult.

### 3.2 Abundance as a function of circular velocity

In this subsection we derive the abundance of model satellites as a function of their circular velocity and compare it to the Local Group data. This is the statistic originally employed by Klypin et al. (1999a) and Moore et al. (1999) to highlight the apparent discrepancy between the CDM cosmogony and the properties of the satellites of the Milky Way. Their motivation for using the distribution of circular velocities of satellite halos is that can be straightforwardly obtained from N-body simulations including only dark matter, whereas the luminosities of satellite galaxies, while fairly easy to measure observationally, cannot be so easily predicted theoretically, because of the complicated dependence on the processes of cooling, star formation, feedback and photoionization. The main drawback of making the comparison in terms of circular velocities is that measuring circular velocities is a difficult task for the majority of the Local Group satellites which do not have gas disks, and in any case these measurements give the circular velocity within the visible galaxy, not the value at the peak of the rotation curve of the dark halo, which is typically what is measured in the simulations. In addition, the comparisons by Klypin

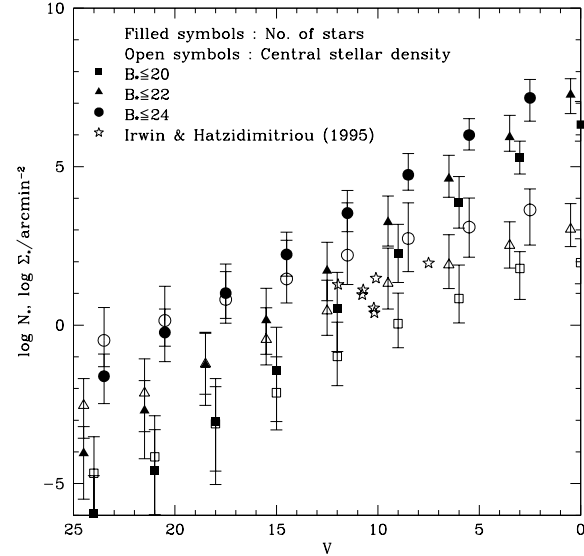


**Figure 3.** The number of stars (filled symbols) and the surface density of stars (open symbols) brighter than  $B_{\star}=20, 22$  and  $24$  (squares, triangles and circles respectively) for satellites of Milky Way type galaxies as a function of the apparent magnitude of the galaxy. The measured central stellar densities for a subset of the Local Group satellites measured by Irwin & Hatzidimitriou (1995), with a limiting magnitude  $B = 22$ , are shown as open stars.

et al. (1999a) and Moore et al. (1999) implicitly assumed a tight relation between subhalo circular velocity and satellite luminosity, since otherwise the observational selection on luminosity modifies the form of the circular velocity distribution, as we will see below.

Before proceeding with the calculation of the satellite circular velocity distribution, it is important to check that our model produces realistic sizes for the satellites, as well as the correct luminosity-circular velocity relation. The size of a galaxy influences the circular velocity because it determines the self-gravity of the visible component (and the associated compression of the halo which we treat using adiabatic invariants, as discussed in Cole et al. 2000). It also determines the part of the rotation curve which is accessible to observations. The luminosity-circular velocity relation enters because, in practice, the distribution of circular velocity is measured for a sample selected to be brighter than a given luminosity.

In Fig. 4 we compare the half-light radii of our model satellites with observations. We estimate the half-light radii of real satellites using published fits to their surface brightness profiles (typically exponentials or King models) in the manner described in detail in the figure caption<sup>§</sup>. For the

<sup>§</sup> For reference, half of the Local Group satellites listed by Mateo (1998), as well as the LMC, SMC and M33, are irregulars and half are spheroidals; for galaxies brighter than  $M_V = -8$ , the model predicts 78% spiral/irregulars and 22% spheroidals. It is likely that the morphological evolution of satellites has been influenced by dynamical processes not included in our model (e.g. Mayer et al. 2001).

model satellites, we take the half-light radius to be the half-mass radius of the stellar system (including both disk and spheroid) that remains within the effective tidal radius. (In Paper I we defined the effective tidal radius as the radius in the original satellite density profile beyond which material has been lost.) We show results for our standard, no photoionization and Cole et al. (2000) models. The sizes of satellites in our standard model are significantly smaller than in the Cole et al. (2000) model, particularly fainter than  $M_V = -15$ . As the figure shows, much of this reduction is due to tidal limitation which strips away the outer layers of the galaxies. Photoionization appears to have little effect on the sizes of satellites. In reality, photoionization does reduce the size, but it also reduces the luminosity, essentially preserving the size-luminosity relation, so that the galaxies typically move in a direction almost parallel to the median relation in Fig. 4. The model predictions are in good agreement with the data and, given the rather crude observational determinations available, this level of agreement seems sufficient at present.

The ‘Tully-Fisher’ relation between the circular velocity and the absolute V-band magnitude of satellites is plotted in Fig. 5. Whenever possible, the circular velocity of real satellites was estimated from the rotation velocity of gas in the ISM (corrected for inclination). Where a measurement of this is not available, we used instead the measured stellar velocity dispersion multiplied by a factor  $\sqrt{3}$ .<sup>¶</sup> For the model satellites, we plot the circular velocity at the stellar half-mass radius, which is typically  $\sim 25\%$  smaller than the peak circular velocity in the tidally limited halo. For the fainter satellites ( $M_V \simeq -10$ ), the circular velocity at the half-mass radius is about half the value at the virial radius, whereas for the brighter satellites ( $M_V \simeq -15$ ), the two are similar. The theoretical relations provide a good description of the data, except in the magnitude range  $-9 \lesssim M_V \lesssim -14$  for which the model velocities are about a factor of 2 too high. In this range, the no photoionization model performs slightly better than the standard model since tidal limitation results in the rotation velocity being measured at a smaller radius, an effect which is offset by the fact that photoionization requires galaxies of fixed luminosity to form in more massive halos when photoionization is switched on (compare the solid and dashed lines in Fig. 5). While it is possible that this discrepancy may reflect a shortcoming of the model, the estimation of circular velocities from current observational data is highly uncertain; improved determinations are extremely important. In addition, there is also some theoretical uncertainty in the calculation of the circular velocity. For example, as noted in Paper I, our model does not account

<sup>¶</sup> The factor  $\sqrt{3}$  follows from the assumption of isotropic stellar orbits in a singular isothermal potential, for a stellar distribution with an  $r^{-3}$  density profile, assumptions which may not be relevant to real galaxies. Alternatively, the average line-of-sight velocity dispersion of the satellite’s spheroid can be estimated by modelling the spheroid as a King profile (which is often a good fit to observed data) and then solving the Jeans equation (see Paper I, eqn. 21). Assuming isotropic orbits, we find  $V_{\text{bulge}} \approx 1.2\sigma_*$  for model satellites, albeit with large scatter, where  $V_{\text{bulge}}$  is the circular velocity of the bulge at the stellar half-mass radius and  $\sigma_*$  is the stellar line-of-sight velocity dispersion. Adopting this latter value does not change our conclusions for the velocity function.

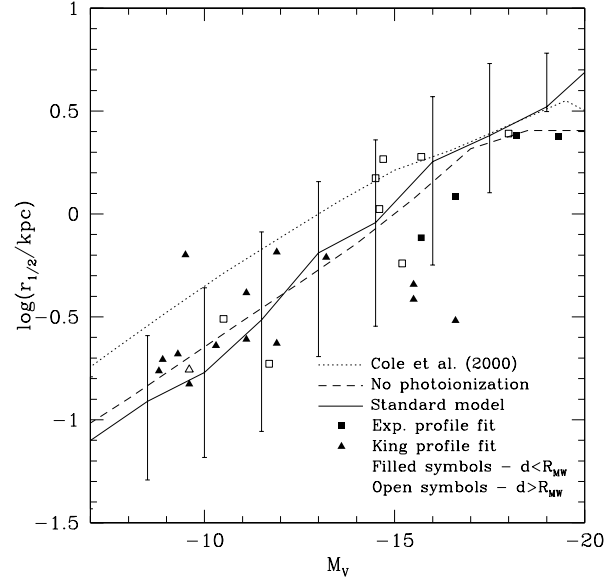


**Figure 4.** The half-light radii of satellite galaxies as a function of absolute V-band magnitude. The points show the radii of the satellites of the Local Group, estimated from the data compiled by Mateo (1998). For spiral and irregular galaxies, we convert their measured exponential scalelength,  $r_{\text{exp}}$ , to a half-light radius by assuming an exponential disk density profile,  $r_{1/2} \approx 1.68r_{\text{exp}}$ ; we show these points as squares. For ellipticals and dwarf spheroidals, we use the quoted parameters of the King (1966) model fits to reconstruct the density profile of the galaxy, and so infer the half-light radius. The core and tidal radii listed by Mateo (1998) are measured along the major axis of each galaxy. We replace these with the equivalent radii for spherically symmetric systems by computing the geometric mean of the radii along the semi-major and semi-minor axes (using the measured ellipticities, which we assume to be independent of radius). These points are shown as triangles. (In the few cases where a galaxy is classed as Irr/dSph, we include it in the Irr class for the purposes of this plot.) Filled points indicate satellites within a distance  $R_{\text{MW}} \approx 270$  kpc from the Milky Way or M31, and open symbols indicate more distant satellites. The solid line corresponds to our standard model, the dashed line to the model that ignores photoionization but which includes tidal stripping of satellite halos, and the dotted line to the Cole et al. (2000) model. The lines show the median relation and the errorbars indicate the 10% and 90% intervals of the distribution in the standard model. In this and subsequent figures errorbars are only shown where the magnitude bin contains enough model galaxies to estimate the 10% and 90% intervals accurately, and so do not appear at the brightest magnitudes. The scatter in the no-photoionization model is similar to this, but in the Cole et al. (2000) model it is typically 60-70% smaller. The half-light radius of the model satellites is taken to be the half-mass radius of the galaxy (including both disk and spheroid) remaining within the effective tidal radius. The half-mass radii of the disk and spheroid prior to tidal limitation were determined in the manner described by Cole et al. (2000).

for changes in the density profile of the satellite after tidal limitation, which may reduce the rotation speed somewhat (Mayer et al. 2001).

The satellite cumulative velocity function is shown in Fig. 6. In our model of photoionization, every dark matter halo whose virial temperature is larger than the minimum temperature for cooling (see Fig. 1 of Paper I) forms a galaxy

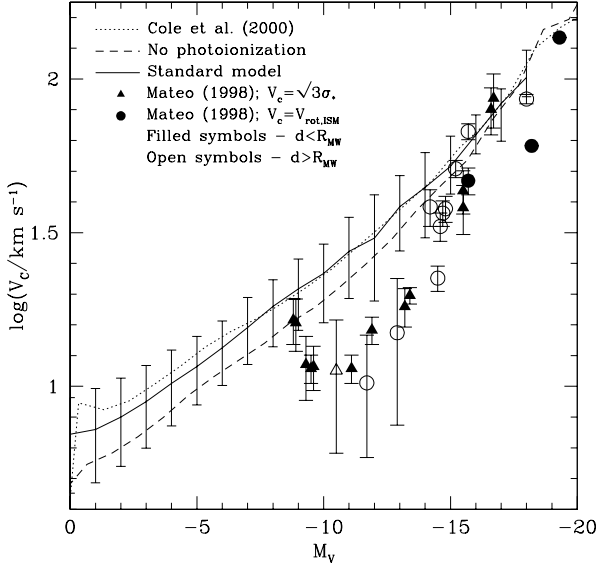


**Figure 5.** The relation between circular velocity and V-band absolute magnitude for satellite galaxies. For the real satellites of the Local Group (Mateo 1998), circles indicate circular velocities inferred from the rotation speed of the ISM, while triangles indicate circular velocities estimated from the stellar velocity dispersion as discussed in the text. Filled symbols denote galaxies within  $R_{MW}$  of the Milky Way or M31, while open symbols denote more distant galaxies. The median relation from our standard model is shown by the solid line with errorbars indicating the 10% and 90% intervals of the distribution. For the model, we plot the circular velocity at the half-mass radius of the satellite (including both disk and spheroid and taking only the mass remaining within the effective tidal radius). The dashed line shows the results from the model in which the effects of photoionization are ignored, but tidal limitation of halos is included, while the dotted line shows the results from the model of Cole et al. (2000). The scatter in the former is similar to that in the standard model, but in the latter it is about 70% of that in the standard model.

(although in low mass halos the galaxies have extremely low mass), and tidal stripping never completely destroys a satellite halo (although halos may be stripped to very small radii). As a consequence, if we naively constructed the full cumulative velocity function of satellites in our model, it would be identical to that of Cole et al. (2000). In reality, many of the satellites in our model are extremely faint either because photoionization severely restricted their supply of star-forming gas, or because tidal stripping removed most of their stars, and so would be unobservable. We therefore apply an absolute magnitude limit to our sample of satellites and construct the cumulative velocity function only for galaxies brighter than this limit. The sample of known Local Group satellites does not have a well-defined absolute magnitude limit (nor an apparent magnitude limit for that matter), but the faintest galaxy listed by Mateo (1998), Draco, has  $M_V = -8.8$ . We therefore choose  $M_V = -9$  as a suitable cut for our models and apply the same cut to the data.

Results for our standard, no photoionization and Cole et al. (2000) models are shown with solid, dashed and dotted lines respectively in Fig. 6. It is immediately apparent that

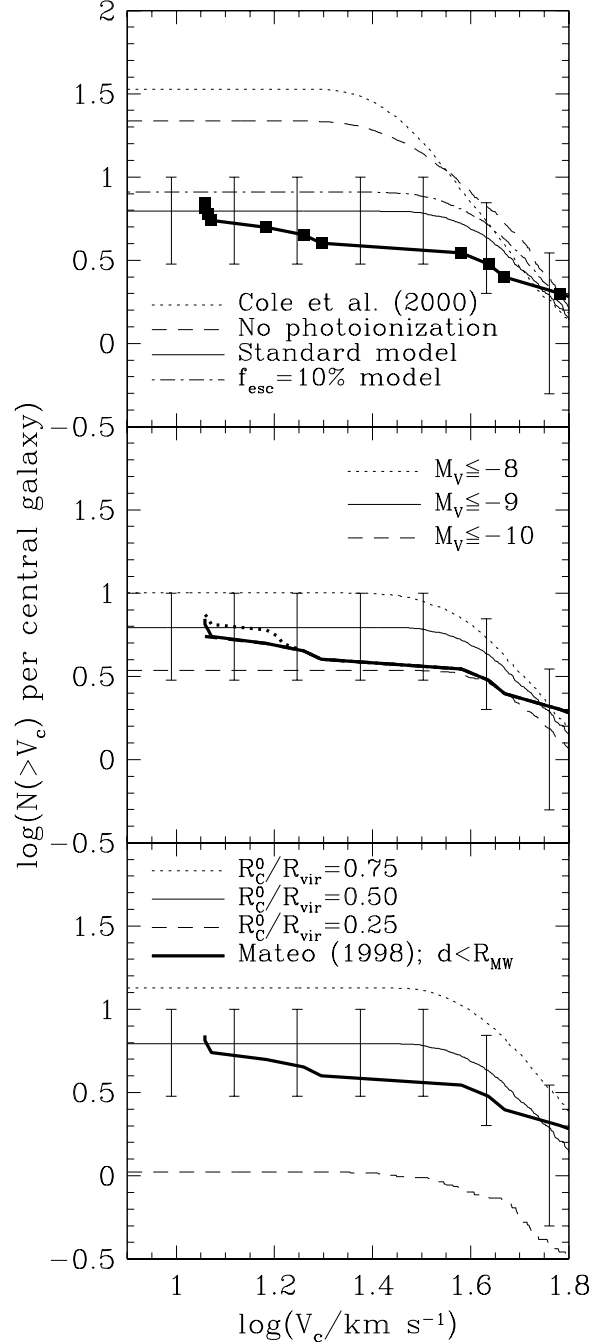


**Figure 6.**

while the model of Cole et al. (2000) substantially overpredicts the number of satellites, our photoionization model is in very good agreement with the data. As the figure clearly shows, the main reduction comes from the effects of photoionization; tidal limitation alone has only a minor effect on the velocity function. The scatter from realization to realization is large: the central 80% of the distribution of velocity functions spans a factor of 3. Adopting a magnitude cut at  $M_V = -10$  produces equally good agreement (except, perhaps, at the lowest circular velocities,  $\lesssim 13\text{km/s}$ ), but taking  $M_V = -8$  leads to roughly twice as many satellites in the



**Figure 6.** (*cont.*) The cumulative velocity function of satellite galaxies. Data for the Local Group per central galaxy (i.e. satellites within  $R_{\text{MW}}$  of the Milky Way or M31), taken from Mateo (1998), are shown by heavy lines without errorbars (in the top panel we also plot squares to indicate the contribution from each individual satellite). *Top panel:* The mean cumulative velocity function of satellites brighter than  $M_V = -9$  in our standard model is shown by the solid line, with errorbars enclosing 10% and 90% of the distribution of velocity functions (from a sample of approximately 70 Milky Way type halos). The circular velocities plotted are measured at the half-mass radius of the combined disk and spheroid system after accounting for tidal limitation. The dot-dashed line shows the effect of reducing  $f_{\text{esc}}$  to 10% (from 100% in the standard model). The dashed line shows the model in which the effects of photoionization are neglected but satellite limitation by tidal stripping is included, while the dotted line corresponds to the model of Cole et al. (2000). The scatter in the former is similar to, and in the latter it is typically 70% of, the scatter in the standard model. All models have  $R_c^0/R_{\text{vir}} = 0.5$ . *Middle panel:* Dependence on the absolute magnitude cut. The thin lines show results for the standard model for the different magnitude cuts: solid for  $M_V = -9$  (as in the top panels), dotted for  $M_V = -8$ , and dashed for  $M_V = -10$ . The thick lines show the Local Group data for the same magnitude cuts, with the same line types (the  $M_V = -10$  line lies almost entirely under the  $M_V = -9$  line). *Lower panel:* As middle panel for the standard model but with different values of  $R_c^0/R_{\text{vir}}$  (as given in the legend);  $R_c^0/R_{\text{vir}}$  is the model parameter that controls the initial orbital radii of satellites as defined in Paper I.

range  $16\text{km/s} \lesssim V_c \lesssim 40\text{km/s}$  as is observed. In all cases, the photoionization model predicts far fewer satellites than the Cole et al. (2000) model. Our results are weakly dependent on the assumed photon escape fraction. The result of assuming  $f_{\text{esc}} = 10\%$  (instead of  $f_{\text{esc}} = 100\%$  in the standard model) is shown by the dot-dashed line in the upper panel. The number of satellites with  $V_c \lesssim 30\text{kms}^{-1}$  is increased by about 25% in this latter case.

Finally we show in the lower panel of Fig. 6 the effect of varying the ratio  $R_c^0/R_{\text{vir}}$ , which parameterizes the initial orbital energy of a satellite in terms of the energy of a circular orbit of radius  $R_c^0$ . In Paper I, we demonstrated that a value of  $R_c^0/R_{\text{vir}} = 0.5$  provides a good match to the number of subhalos seen in high-resolution N-body simulations, and is comparable to the mean value measured for satellites in those simulations at  $z = 0$ . Increasing  $R_c^0/R_{\text{vir}}$  to 0.75 produces somewhat too many satellites, while reducing it to 0.25 seriously underpredicts the number of satellites. Increasing  $R_c^0/R_{\text{vir}}$  makes satellite orbits begin at larger radii where tidal forces are weaker and so allows more satellites to survive (decreasing  $R_c^0/R_{\text{vir}}$  has the opposite effect). The magnitude of the changes induced by adopting these alternative values for  $R_c^0/R_{\text{vir}}$  is comparable to that seen for calculations of satellite halo abundances in the pure dark matter calculations reported in Paper I, and so can be seen to be due almost entirely to the enhanced(reduced) tidal limitation and dynamical friction resulting from a smaller(larger) value of  $R_c^0/R_{\text{vir}}$ , supplemented slightly by changes in the luminosities of satellites which alter whether they meet our selection criteria for this figure.

The exact distribution of  $R_c^0/R_{\text{vir}}$  is therefore very important, and would be worth determining accurately from numerical simulations. We stress that the value  $R_c^0/R_{\text{vir}} =$

0.5 was chosen to match the results of N-body simulations of dark matter, and also results in good agreement with the abundances of satellite galaxies.

## 4 OTHER PROPERTIES OF SATELLITES

In addition to the abundance, our model of galaxy formation predicts many other properties of the satellite galaxy population and their associated dark halos. We now explore some of them, particularly those for which observational data are available.

### 4.1 Gas content, star formation rates, metallicities and colours

We begin by considering the gaseous content and star formation rates of satellites. The mass of hydrogen (atomic plus molecular), normalized to the V-band luminosity, is shown, as a function of V-band magnitude, in Fig. 7. A rapid decline in the gas content towards faint magnitudes is predicted by the models. This is a direct consequence of the strong effects of supernova feedback in faint, low mass galaxies which efficiently eject much of their cold gas and rapidly consume any remaining fuel (these galaxies, being satellites, are unable to accrete fresh gas in our model). The observational data show a band of almost constant gas-to-luminosity ratio which is occupied exclusively by galaxies beyond  $R_{\text{MW}}$  of the Milky Way or M31 at faint magnitudes. Galaxies within  $R_{\text{MW}}$  frequently have only upper limits to their gas mass. Our model predictions are consistent with the observations but, since the data often consist only of upper limits, this comparison is not particularly conclusive.

We now consider the star formation rates in satellites as estimated from their  $\text{H}\alpha$  luminosities. In Fig. 8, we plot the  $\text{H}\alpha$  luminosity per unit hydrogen mass for satellites with measurements or limits on  $\text{H}\alpha$  (all such galaxies also have measured gas masses). With so few data points (note that many of the galaxies in the plot lie further than  $R_{\text{MW}}$  from the Milky Way or M31), it is difficult to quantify the level of agreement between model and data. Of the six satellites within  $R_{\text{MW}}$  with measured  $\text{H}\alpha$  luminosity, four lie close to the model prediction, while one fainter satellite has an  $\text{H}\alpha$  to hydrogen ratio an order of magnitude above the model relation, and another has an upper limit lying three orders of magnitude below the model expectation.

In Fig. 9, we plot the metallicity of the ISM gas (upper panel) and of the stars (lower panel). In both cases, the Local Group satellites exhibit a trend of increasing metallicity with luminosity. Our models show a trend in the same sense, although for the ISM it appears somewhat weaker than for the data. It is interesting that the satellites within  $R_{\text{MW}}$  lie much closer to the model predictions (which are only for satellites within Milky Way-like halos) than those outside  $R_{\text{MW}}$ , but with the limited data available it is impossible to say if this is a significant effect. The stellar metallicities in the model also agree well with the data, except perhaps at the faintest magnitudes where the model is slightly too high. While photoionization makes little difference to the metallicities of galaxies brighter than  $M_V \approx -15$ , at fainter magnitudes the standard model predicts slightly higher metallicities than the Cole et al. (2000) model. Photoionization

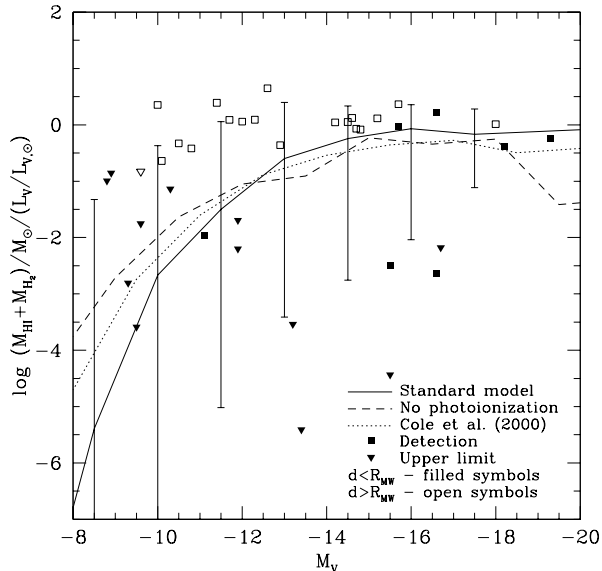


**Figure 7.** The mass of hydrogen per unit V-band luminosity in satellite galaxies as a function of V-band absolute magnitude. Data for the Local Group satellites are taken from Mateo (1998), except for the LMC and SMC for which HI masses are taken from Westerland (1997), M33 for which the HI mass comes from Corbelli & Salucci (2000) and for NGC3109 and Antlia for which HI masses are taken from Barnes & de Blok (2001). HI detections are shown as squares, and upper limits as triangles. Galaxies within  $R_{MW}$  of the Milky Way or M31 are represented by filled symbols and more distant satellites by open symbols. Solid, dashed and dotted lines show results from our standard, no photoionization and Cole et al. (2000) models respectively. The lines show the median model relations and the errorbars indicate the 10% and 90% intervals of the distribution in the standard model. The scatter in the other models is comparable to this.

causes galaxies of a given absolute magnitude to form in higher circular velocity halos. These have deeper potential wells which reduce the effectiveness with which supernovae feedback expels gas, thus increasing the effective yield (see Cole et al. 2000) and resulting in a higher metallicity. In Paper I, we considered the metallicity of the ISM for galaxies in general and found that photoionization actually reduced the gas metallicity in faint galaxies by preventing pre-processing of that gas in smaller halos. In the case of satellites, photoionization has a much smaller effect because, unlike central galaxies, the satellites are not accreting gas at present, and so their metallicity is much less sensitive to any pre-enrichment.

Finally, we consider the B-V colours of satellite galaxies. These are plotted in Fig 10 for the Local Group, as a function of satellite V-band absolute magnitude and compared with the model predictions. The model predictions are rather insensitive to whether or not photoionization is included. With or without photoionization, satellites are typically very old systems with little recent star formation and so their colours correspond to those of an old ( $\gtrsim 10$  Gyr), low metallicity stellar population (i.e. roughly  $B-V=0.5-0.7$  for the IMF considered here). Filled squares in the figure indicate Local Group satellites within  $R_{MW}$  of the Milky Way or M31. The colours of these galaxies are in good agreement with

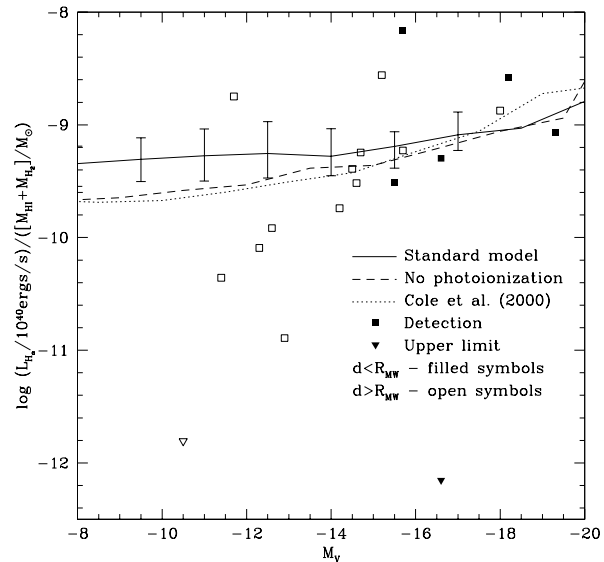


**Figure 8.** The  $H\alpha$  luminosity per unit mass of hydrogen for satellite galaxies, as function of absolute V-band magnitude. Symbols show values for Local Group satellites taken from Mateo (1998) and from Westerland (1997) for the Magellanic Clouds and Kenicutt (1998) for M33. Satellites within  $R_{MW}$  of the Milky Way or M31 are shown as filled symbols, with more distant satellites shown as open symbols.  $H\alpha$  detections are denoted by squares, and upper limits by triangles. Solid, dashed and dotted lines indicate results from our standard, no photoionization and Cole et al. (2000) models respectively. The lines indicate the median relation and the errorbars the 10% and 90% intervals of the distribution in the standard model. The scatter in the other models is comparable to this.

the model predictions, except perhaps for two intrinsically faint galaxies for which the observed colours are very uncertain. Interestingly, Local Group galaxies which lie beyond  $R_{MW}$  of either the Milky Way or M31 have systematically bluer colours, suggesting that they have experienced recent star formation. This is generically expected in our model because these objects are still the central galaxies in their host halos and, unlike genuine satellites, they are still able to accrete gas to fuel star formation even at the present day. This interpretation is consistent with the higher overall gas content measured in the most distant galaxies as seen in Fig. 7

## 4.2 Structure

Dynamical quantities describing the structure of satellite galaxies and their dark matter halos are readily available in our model of galaxy formation. In Fig. 11, we show some of these quantities as a function of the absolute V-band magnitude of the satellite. We remind the reader that in our calculations, the dynamical and structural properties of the satellite halos within the effective tidal radius are unaffected by the mass loss beyond that radius. In the upper panels, we plot the circular velocity at the virial radius (left-hand panel) and at the NFW scale radius (right-hand panel). The virial radius and corresponding circular velocity here are the values the satellite halo last had when it was still a separate

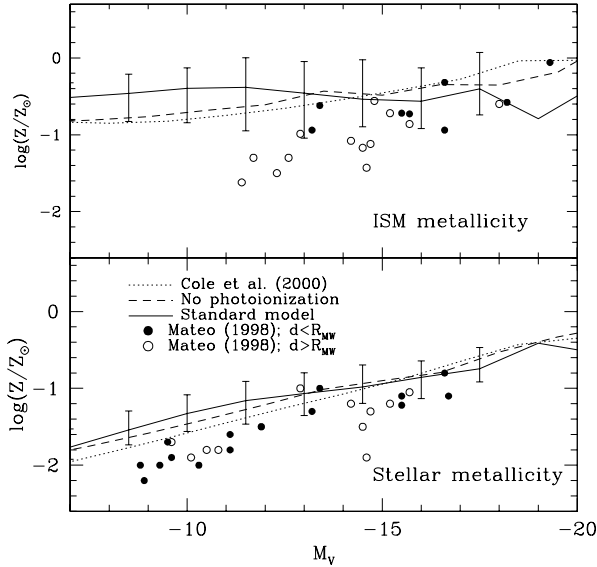


**Figure 9.** The metallicity of satellite galaxies as a function of absolute V-band magnitude. Metallicities for Local Group satellites are taken from Mateo (1998), except for the Magellanic Clouds (Skillman, Kennicutt & Hodge 1989) and M33 (Kobulnicky, Kennicutt & Pizagno 1999). The upper panel shows the metallicity of gas in the ISM (relative to Solar, with  $Z_{\odot} = 0.02$ ), while the lower panel shows the metallicity of the stars. Filled circles indicate satellites within  $R_{\text{MW}} \approx 270$  kpc of the Milky Way or M31, with more distant satellites shown as open circles. Solid lines give the median relation in our standard model, with error bars indicating the 10% and 90% intervals. Dashed lines correspond to our no photoionization model (which includes tidal stripping of satellites) and dotted lines to the Cole et al. (2000) model. The scatter in these models is comparable to that in the standard model.

halo, before it merged with the Milky Way halo. In evaluating the circular velocity, we take into account contributions from both dark and baryonic matter in the galaxy, including the contraction of the dark halo caused by the condensation of the galaxy (which is assumed to proceed adiabatically). For fainter satellites, the photoionization model predicts significantly higher circular velocities than the other models. The reason for this is one we have encountered before: the inhibiting effect of photoionization leads to satellites of a given luminosity forming in a more massive halo than would be the case in the absence of photoionization. Note that such an effect is not seen in Fig. 5 where we plotted the satellite galaxy “Tully-Fisher” relation. There, the increase in circular velocity is offset by the reduction in the sizes of galaxies, which causes the visible matter to sample the rotation curve at smaller radii where the circular velocity is less.

In the lower left-hand panel of Fig. 11, we plot the effective tidal radii, as defined above and in Paper I, of the satellites<sup>||</sup>. For comparison, we plot the virial radius of the

<sup>||</sup> In our calculations, galaxies are modelled with surface density profiles which initially extend to the virial radius of the halo in which they formed. We can therefore define a tidal radius for satellites even if this turns out to be much larger than the visible extent of the galaxy. In practice, when this occurs, the tidal radius

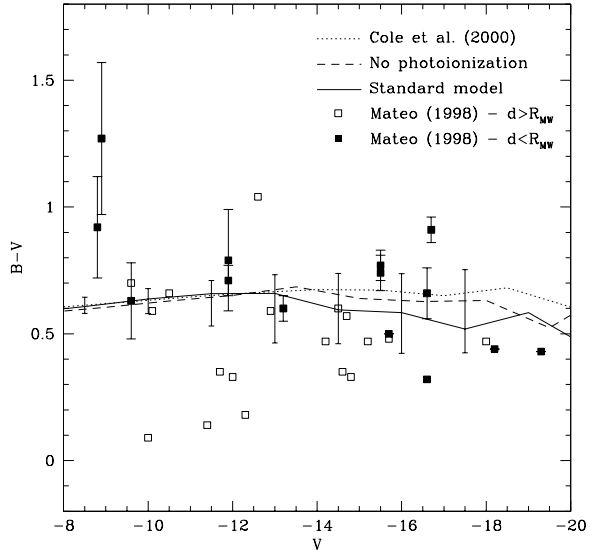


**Figure 10.** The B-V colour of satellite galaxies as a function of absolute V-band magnitude. Colours for Local Group satellites are taken from Mateo (1998), except for the Magellanic Clouds (Skillman, Kennicutt & Hodge 1989) and M33 (Kobulnicky, Kennicutt & Pizagno 1999). Filled squares indicate satellites within  $R_{\text{MW}} \approx 270$  kpc of the Milky Way or M31, with more distant satellites shown as open squares. The solid line gives the median relation in our standard model, with error bars indicating the 10% and 90% intervals. The dashed line corresponds to our no photoionization model (which includes tidal stripping of satellites) and the dotted line to the Cole et al. (2000) model. The scatter in these models is comparable to that in the standard model.

halo in the Cole et al. (2000) model, which does not include tidal limitation (and assumes, for calculations of dynamical friction, that the satellite retains all of its halo after it merges with a large halo). Tidal forces strip the halos of the faintest galaxies to less than 10% of their initial virial radius, but this effect becomes much less dramatic for the brighter galaxies. (The virial radii of the halos harbouring satellites of a given  $M_V$  are actually slightly larger than the values given by the Cole et al. (2000) model since photoionization causes galaxies of fixed  $M_V$  to form in larger halos). In the lower right-hand panel, we show the NFW scale radius of the halos (lower set of lines). For comparison, we also show the median virial radius (i.e. the virial radius of the satellite’s halo before it merged with the Milky Way’s halo; upper set of lines). Comparison of the two shows that satellites typically formed in halos with concentration parameters in the range  $c = 5-6$ .

## 5 DISCUSSION

Small satellite galaxies like those that surround the Milky Way are the descendants of some of the oldest objects in the Universe. Thus, to understand their properties, it is necessary to take into account processes that occurred at very

plotted should be considered to be the tidal radius of the satellite’s halo rather than that of the satellite itself.

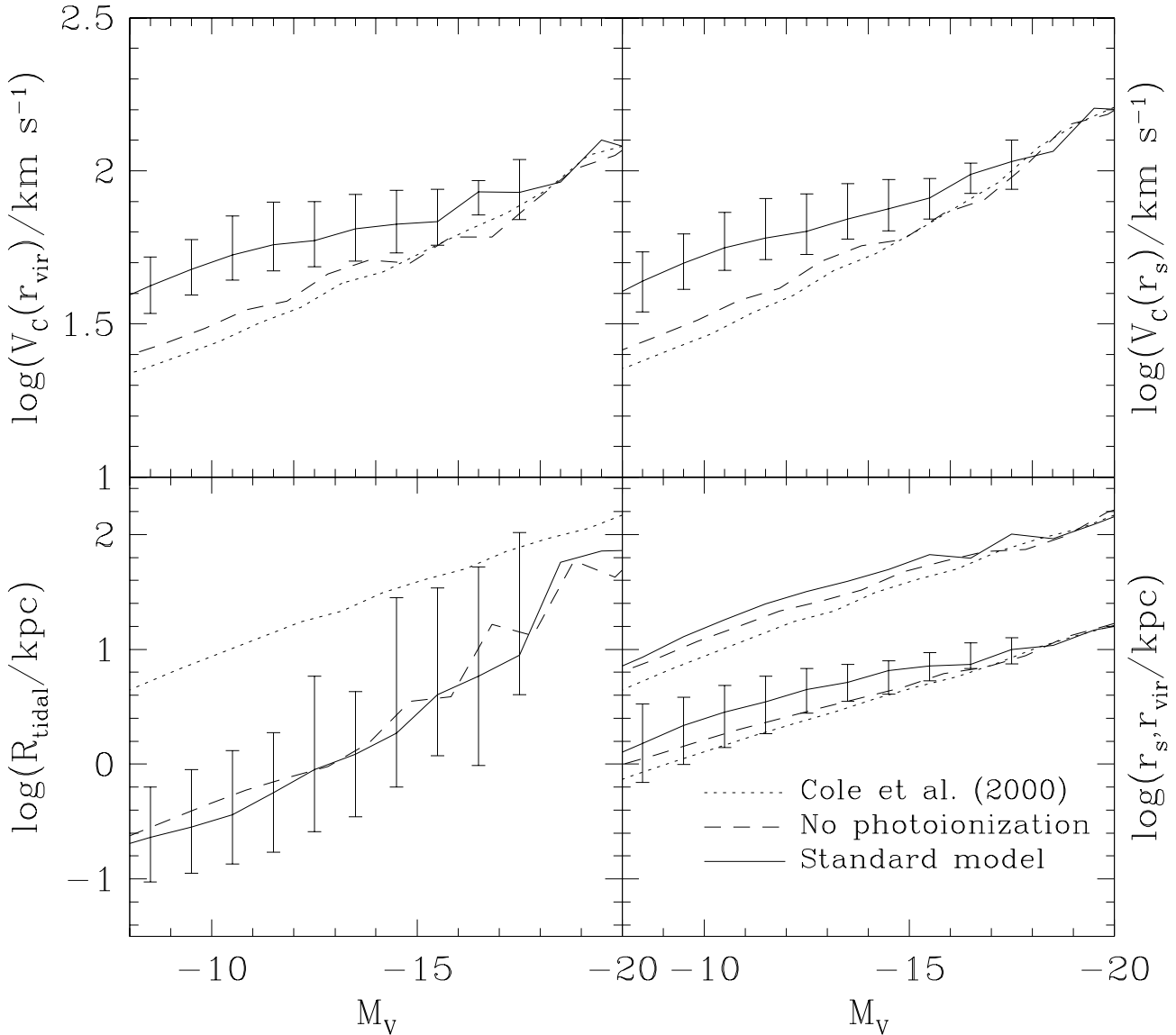


**Figure 11.** Predicted dynamical and structural properties of satellite galaxies and their dark matter halos, as a function of the absolute V-band magnitude of the satellite. In all the panels, the lines show the median model relation: solid lines for the standard model, dashed lines for no-photoionization model (which, however, includes tidal stripping of the satellites) and dotted lines for the Cole et al. (2000) model. As before, the errorbars indicate the 10% and 90% intervals of the distribution in the standard model; the scatter in the other two models is comparable. *Upper left:* The circular velocity at the virial radius. *Upper right:* The circular velocity at the NFW scale radius,  $r_s$ . This takes into account contributions from both dark and baryonic matter in the galaxy, including the contraction of the dark halo caused by the condensation of the galaxy (assumed to proceed adiabatically). *Lower left:* The effective tidal radii of the satellites. For the Cole et al. (2000) model, which does not include tidal limitation, we plot instead the virial radius of the halo for comparison. *Lower right:* The NFW scale radius of the satellite halos (lower set of lines) and the virial radius of the halos (upper set of lines).

early times, like the reionization of the Universe, which are often neglected when studying the properties of larger galaxies. Furthermore, since these satellites orbit in the halo of the parent galaxy, it is also important to take into account dynamical processes such as tidal effects and dynamical friction. We have used an extension of the Cole et al. (2000) semi-analytic model of galaxy formation which includes all these processes to study the expected abundance and properties of satellite galaxies in the Local Group. Our work im-

proves upon earlier studies by Kauffmann, White & Guiderdoni (1993) and Bullock, Kravtsov & Weinberg (2000) because it self-consistently calculates the physics of reionization and galaxy formation and includes a treatment of the main dynamical effects experienced by satellites orbiting in a dark matter halo.

We generated samples of halos containing galaxies similar to the Milky Way. Photoionization, which occurs at  $z \approx 8$ , inhibits the formation of small galaxies and so the

satellites that survive to the present tend to be those that formed while the universe was still neutral. This has the consequence of greatly suppressing the number of satellites of a given luminosity relative to the number that would be expected if photoionization were neglected. Furthermore, at a given satellite luminosity, we find that it is those satellites with the lowest circular velocity that are preferentially depleted by the effects of photoionization. The measured distribution function of satellite circular velocity depends on this differential destruction but also on the internal structure of the satellite which determines the shape of its rotation curve. We take the ‘measured’ circular velocity of a satellite to be the value at the half-light radius. We find that for the fainter satellites ( $M_V \simeq -10$ ), the measured circular velocity is about half the value at the virial radius because the half-light radius is within the rising part of the rotation curve, whereas for the brighter satellites ( $M_V \simeq -15$ ), the measured circular velocity is very similar to the value at the virial radius. These effects work together to produce both a luminosity function and a circular velocity function which are in good agreement with the available data. This result is remarkable because we have not had to adjust a single parameter value in the Cole et al. (2000) model nor fine-tune our treatment of photoionization.

Our model also predicts the sizes and metallicities of satellites and these also turn out to be in good agreement with the limited amount of data currently available. The model predicts that photoionization has negligible effects in galaxies with circular velocity above about  $60 \text{ km s}^{-1}$ , in agreement with earlier analytical (Efstathiou 1992; Thoul & Weinberg 1996) and numerical treatments (Quinn, Katz & Efstathiou 1996; Navarro & Steinmetz 1997).

Our model can, in principle, be tested on the basis of the predictions it makes for as yet unobserved properties of the satellite population in the Local Group. In particular, our model suggests that there should be a large population of faint satellites around the Milky Way awaiting discovery. A near complete census would require deep imaging (at least to 26 V-band magnitudes per square arcsecond). Alternatively, satellites may be recognized as an excess of stars against the background. We have presented detailed predictions for the expected number of stars and their surface density as a function of the luminosity of the satellite to which they belong. These calculations may be useful in designing observational strategies aimed at discovering new satellites. A further possibility is to try and detect these satellites by searching for their HI content (Putman et al. 2001). Our model predicts that  $M_V = -10$  satellites should typically contain  $10^5 M_\odot$  of HI, with a rapid decline in HI mass at fainter magnitudes. Such observations are difficult, but perhaps not impossible.

We conclude that speculative mechanisms such as non-standard inflation (Kamionkowski & Liddle 2000) or new components of the Universe such as warm, self-interacting or annihilating dark matter (Hogan 1999; Spergel & Steinhardt 2000; Yoshida et al. 2001; Craig & Davis 2001) are not required to explain the observed abundance of Local Group satellites. Instead, the low abundance of satellites is a natural consequence of galaxy formation in a CDM universe when the physical effects of photoionization and tidal interactions, two processes which are known to occur, are taken into account. Continuing improvement in the observational data for Local Group galaxies, particularly better

measurements of their structure and dynamical state and an assessment of the completeness of existing samples, together with searches for new satellites, will provide a strong test of current models of galaxy formation.

## ACKNOWLEDGMENTS

CSF acknowledges a Leverhulme Research Fellowship. CGL acknowledges support at SISSA from COFIN funds from MURST and funds from ASI. CMB acknowledges a Royal Society University Research Fellowship. SMC acknowledges a PPARC Advanced Fellowship. We also thank Ben Moore for drawing our attention to the Milky Way satellite problem.

## REFERENCES

- Abel T., Mo H. 1998, *ApJL*, 494, 151  
 Babul A., Rees M. J. 1992, *MNRAS*, 255, 346  
 Barkana R., Loeb A., 1999, *ApJ*, 523, 54  
 Barnes D. G., de Blok W. J. G., 2001, *astro-ph/0107474*  
 Baugh C. M., Cole S., Frenk C. S., 1996, *MNRAS*, 283, 1361  
 Benson A. J., Lacey C. G., Baugh C. M., Cole S., Frenk C. S., 2001, *MNRAS*, submitted (Paper I)  
 Binney J., Merrifield M., 1998, “Galactic Astronomy”, Princeton University Press  
 Bond J. R., Cole S., Efstathiou G., Kaiser N., 1991, *ApJ*, 379, 440  
 Bower R. G., 1991, *MNRAS*, 248, 332  
 Bullock J. S., Kravtsov A. V., Weinberg D. H., 2000, *ApJ*, 539, 517  
 Burkert A., 1995, *ApJ*, 447, L25  
 Cole S., 1991, *ApJ*, 367, 45 *MNRAS*, 281, 716  
 Cole S., Lacey C. G., Baugh C. M., Frenk C. S., 2000, *MNRAS*, 319, 168  
 Corbelli E., Salucci P., 2000, *MNRAS*, 311, 441  
 Craig M. W., Davis M., 2001, *New Astr.*, in press (*astro-ph/0106542*)  
 Dehnen W., Binney J., 1998, *MNRAS*, 294, 429  
 Dekel A., Silk J., 1986, *ApJ*, 303, 39  
 Efstathiou G., 1992, *MNRAS*, 256, 43p  
 Fan X. et al. (The SDSS Collaboration), 2000, *AJ*, 120, 1167  
 Flores R. A., Primack J. R., 1994, *ApJ*, 427, L1  
 Gnedin N. Y., 2000, *ApJ*, 542, 535  
 Hogan C., 1999, in the Proceedings of the NATO Advanced Study Institute on Astrofundamental Physcs, eds. N. Sanchez and A. Zichichi  
 Irwin M., Hatzidimitriou D., 1995, *MNRAS*, 277, 1354  
 Kamionkowski M., Liddle A. R., 2000, *Phys. Rev. Lett.*, 84, 4525  
 Katz N., Weinberg D. H., Hernquist L., 1996, *ApJS*, 105, 19  
 Kauffmann G., White, S. D. M., Guiderdoni, B., 1993, *MNRAS*, 264, 201  
 Kennicutt R. C., 1983, *ApJ*, 272, 54  
 Kennicutt R., 1998, *ApJ*, 498, 541  
 Kepner J. V., Babul A., Spergel D. N. 1997, *ApJ*, 487, 61  
 King I. R., 1966, *AJ*, 71, 64  
 Klypin A., A., Kravtsov A. V., Valenzuela O., Prada F., 1999a, *ApJ*, 522, 82  
 Kobulnicky H. A., Kennicutt R. C., Pizagno J. L., 1999, *ApJ*, 514, 544  
 Kravtsov A. V., Klypin A. A., Bullcock J. S., Primack J. R., 1998, *ApJ*, 502, 48  
 Lacey, C.G., Silk, J., 1991, *ApJ*, 381, 14  
 Leitherer C., Ferguson H., Heckman T. M., Lowenthal J. D., 1995, *ApJ*, 454, 19

- Lejeune T., Schaerer D., 2001, *A&A*, 366, 538  
Madau P., Haardt F., Rees M. J., 1999, *ApJ*, 514, 648  
Matthewson D. S., Ford V. L., Buchhorn M., 1992, *ApJS*, 81, 413  
Mateo M. L., 1998, *ARA&A*, 36, 435  
Mayer L., Governato F., Colpi M., Moore B., Quinn T., Wadsley J., Stadel J., Lake G., 2001, *ApJ* in press (astro-ph/0103430)  
Moore B., 1994, *Nat.*, 370, 629  
Moore B., 2001, to appear in Proceedings of the Texas Symposium astro-ph/0103100  
Moore B., Ghigna S., Governato F., Lake G., Quinn T., Stadel J., Tozzi P., 1999, *ApJ*, 524, 19  
Moore B., Gelato S., Jenkins A., Pearce F. R. & Quilis V. 2000, *ApJ*, 535, L21  
Navarro J. F., Frenk C. S., White S. D. M., 1997, *ApJ*, 490, 493  
Navarro J. F. & Steinmetz, M., *ApJ*, 478, 13  
Putman M. E. et al., in preparation  
Quinn T., Katz N., Efstathiou G., 1996, *MNRAS*, 278, 49  
Rees M. J. 1986, *MNRAS*, 218, 25  
Skillman E. D., Kennicutt R. C., Hodge P. W., 1989, *ApJ*, 347, 875  
Shapiro P. R., Giroux M. L., Babul A. 1994, *ApJ*, 427, 25  
Somerville R. S., 2001, astro-ph/0107507  
Spergel D. N., Steinhardt P. J., 2000, *Ph. Rv. L.*, 84, 3760  
Steidel C. C., Pettini M., Adelberger K. L., 2001, *ApJ*, 546, 665  
Taylor J. E., Babul A., 2000, astro-ph/0012305  
Thoul A. A., Weinberg D. H., 1996, *ApJ*, 465, 608  
Weinberg M. D., Hernquist, L. & Katz, N. 1997, *ApJ*, 477, 8  
Westerlund B. E., 1997, "The Magellanic Clouds", Cambridge Astrophysics Series, No. 29, Cambridge University Press  
White S. D. M., Rees M. J., 1978, *MNRAS*, 183, 341  
White S. D. M., Frenk C. S., 1991, *ApJ*, 379, 52  
Yoshida N., Springel V., White S.D.M., Tormen G., 2001, *ApJ* in press, astro-ph/0006134